3

Comparative Study of Dye-Sensitized Solar Cell Based on ZnO and TiO_2 Nanostructures

Y. Chergui, N. Nehaoua and D. E. Mekki
Physics Department, LESIMS Laboratory,
Badji Mokhtar University, Annaba,
Algeria

1. Introduction

The dye-sensitized solar cell (DSC) is a third generation photovoltaic device that holds significant promise for the inexpensive conversion of solar energy to electrical energy, because of the use of inexpensive materials and a relatively simple fabrication process. The DSC is based on a nano-structured, meso-porous metal oxide film, sensitized to the visible light by an adsorbed molecular dye. The dye molecules absorb visible light, and inject electrons from the excited state into the metal oxide conduction band. The injected electrons travel through the nanostructured film to the current collector, and the dye is regenerated by an electron donor in the electrolyte solution. The DSC is fully regenerative, and the electron donor is again obtained by electron transfer to the electron acceptor at the counter electrode (Ito et al, 2006). The current certified efficiency recordis11.1% for small cells, and several large-scale tests have been conducted that illustrate the promise for commercial application of the DSC concept. A schematic presentation of the operating principles of the DSC is given in Figure1. At the heart of the system is a mesoporous oxide layer composed of nanometer-sized particles which have been sintered together to allow for electronic conduction to take place. The material of choice has been TiO_2 (anatase) although alternative wide band gap oxides such as ZnO, and Nb_2O_5 have also been investigated. Attached to the surface of the nanocrystalline film is a monolayer of the charge transfer dye (Janne, 2002).
Nanocrystalline electronic junctions compose of a network of mesoscopic oxide or chalcogenide particles, such as TiO_2, ZnO, Fe_2O_3, Nb_2O_5, WO_3, Ta_2O_5 or Cds and CdSe, which are interconnected to allow for electronic conduction to take place. The oxide material of choice for many of these systems has been TiO_2. Its properties are intimately linked to the material content, chemical composition, structure and surface morphology. From the point of the material content and morphology, two crystalline forms of TiO_2 are important, anatase and rutile (the third form, brookite, is difficult to obtain). Anatase is the low temperature stable form and gives mesoscopic films that are transparent and colorless (Fang et al, 2010).
The application of ZnO in excitonic solar cells, XSCs, (organic, dye sensitized and hybrid) has been rising over the last few years due to its similarities with the most studied semiconductor oxide, TiO_2. ZnO presents comparable bandgap values and conduction band position as well as higher electron mobility than TiO_2. It can be synthesized in a wide variety of nanoforms applying straight forward and scalable synthesis methodologies.

Particularly, the application of vertically-aligned ZnO nanostructures it is thought to improve contact between the donor and acceptor material in organic solar cells (OSCs), or improve electron injection in dye sensitized solar cells (DSCs).7 To date, DSC based on ZnO have achieved promising power conversion efficiency values of 6%.

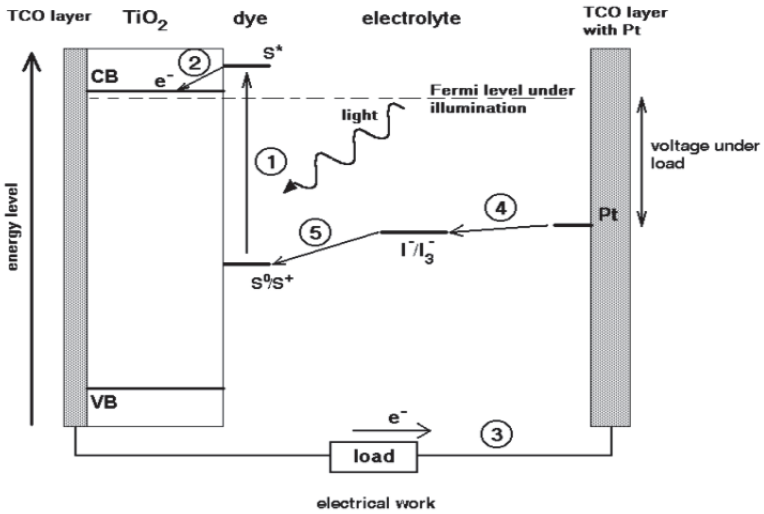

Fig. 1. Principle of operation and energy level scheme of the dye-sensitizednanocrystalline solar cell. Photo-excitation of the sensitizer (S) is followed by electron injection into the conduction band of the mesoporous oxidesemiconductor. The dye molecule is regenerated by the redox system, which itself is regenerated at the counter electrode by electrons passed through the load. Potentials are referred to the normal hydrogen electrode (NHE). The open-circuit voltage of the solar cell corresponds to the difference between the redox potential of the mediator and the Fermi level of the nanocrystallline film indicated with a dashed line (janne, 2002).

lthough most of the reported works on DSSC are based on TiO_2 porous thin films, various structures of ZnO are also being used for DSSC fabrication. The advantages of using ZnO over TiO_2 are its direct band gap (3.37 eV), higher exciton binding energy (60 meV) compared to TiO_2 (4 meV), and higher electron mobility (200 $cm^2 V^{-1} s^{-1}$) over TiO_2 (30 $cm^2V^{-1} s^{-1}$). However, the efficiency of the DSSC based on ZnO nanostructures is still very low (5%). Here we present a comparative study between ZnO and TiO_2 dye-sensitized solar cell (DSSC) by comparing its efficiency, fill factor, the current of short circuit I_{sc} and voltage of open circuit V_{oc} (Jingbin et al, 2010).

2. Materials

2.1 ZnO presentation

ZnO is an envirenment-friendly material (Myo et al, 2008), is a rogarded as one of the most promising substitution materials, and much interest has been paid to semiconductor nanostructures. Too, ZnO is one of the most important functional semi-conductor and is a very attractive material for application devices.

Zno is an environment-friendly material, is a promising candidate for exciton-related optoelctronic devices in the ultraviolet region, and it is also applicable to the devices based in reduced dimensional quantum effect because it can be grown in various crystalline form with submicron size such as whiskers, nanobelts, nanorods, nanowires, nanoplatelets, and so on. ZnO is a regarded as one of the most promising substitution materials for ITO (Introdium Thin Fims)today because of its good resistivity, high transmittance, nontoxicity, and low const. However pure ZnO thin films have a lower electric conductivity than ITO thin fims (You-Seung et al, 2008).

Recently, hollow micro/nanostructures have become of great interst because of their excellent characteristics such as density , high surface-to-volume ratio, and how coefficient sof thermal expansion and refractive index, which makes them attractive for applications ranging from catalystsupports, anti-reflection surface coatings, microwaves absorption (Lou et al, 2008; Zhong et al, 2000) , encapsulating sentive materials (Li et al, 2005; Dinsmore et al, 2002), drug delivery, and rechargeable batteries (Liang et al, 2004; Lee et al, 2003).

Rapid developments in the synthesis of hollow structures, such as CuO (Wang. et al, In press; Liu et al, 2009 Cu_2O (Teo et al, 2006; Chang et al , 2005), TiO_2 (Yu et al, 2007), SnO_2 (Cao et al, 2006; Wang et al, 2006), Fe_2O_3(Liu et al, 2009), Co_3O_4 (Park et al, 2009; Zhao et al, 2008), β-$Ni(OH)_2$ (Wang et al, 2005), α-MnO_2 (Li et al, 2006), CuS (Liu et al, 2007; Yu et 2000), Sb_2S_3 (Cao et al, 2006), ZnO (Zhou et al. 2007; Lin, et al, 2009), $CdMoO_4$(Wang et al, 2009; Wang et al, 2006), and $ZnWO_4$ (Huang et al, 2006), have greatly advanced our ability to tune their mechanical, optical, electrical, and chemical properties to satisfy the various needs of practical applications.

ZnO can be useful in many fields, such as in the rubber industry (Ibarra et al, 2002), photocatalysis(Hsu et al, 2005), sunthesis of ZnO (Hsu et al, 2005; Sun et al, 2007; Zhang et al, 2005). Cosmetic and pharmaceutical industries, and for therapeutic applications (Rosenthal et al, 2008), but little work have been done in these areas (Rosenthalet al, 2008; Chen et al, 2009; Pal et al, 2009). ZnO, as a wide gape semiconductor material, is becoming an increasing concern because of its biocompatibility, nontoxity, and good mechanical, optical, electrical properties. Thus, research about ZnO_2 and ZnO hollow spheres is of great importance and should be paid more attention (Ceng et al, 2009).

ZnO nanoparticules and quantium dots technologically important owing to their special properties and potential use in the fabrication of sensors, light emitters operating in the short-wavelegth range from blue to ultraviolet, transparent conducting oxides, and solar cells (özgör et al, 2005; Sakurai et al, 2002; Th et al, 2003).

Both high-quality p-and n-type ZnO thin films play an important role in the fabrication of optical devices. The production of ZnO with an n-type doping is simple without the need for intentional doping (Toshiya et al, 2008).

ZnO is expected to be one of the candidate host materials for impurity doping (Yamamoto et al, 2005; Ishizumi et al, 2005). However the optical properties of impurity-doped ZnO nanostructures are not well understood. very recently highly porous ZnO films have been successfully fabricated by electrodeposition using eosin Y(EY)dye molecules (T. Yoshida et al, 2003; T. Yoshida et al, 2004), and various lanthanoide ions were introduced into the films. (Pauporté et al, 2006). This fabrication method has been applied to high-efficiency dye-sensitized solar cells (Yoshida et al, 2004).

The application of ZnO inexcitonic solar cells, XSCs (organic, dye sensitized and hybrid) has been rising over the last few years due to its similarities with most studied semiconductor

oxide, TiO_2. ZnO presents comparable band gap value and conduction band position as well as higher electron mobility than TiO_2 (Quintana et al, 2007; Keis et al, 2002). It can be synthesized in a wide variety of nanoforms (Wang, et al, 2004) applying strainght forward and scalable synthesized methodologies (Fan et al, 2006; Greene et al, 2003). particularly, the application of vertically-alligned ZnO NANOSTRUCTURES it is thought to improve contact between the donor and acceptor material in organic solar cells (OSCs), or improve electron injection in dye sensitized solar cells (DSCs) (Gonzalez et al, 2009) To date, DSC based on ZnO have achieved promising power conversion efficiency values of ~6%.(Keis et al, 2002; Yoshida et al, 2009).

Yet ZnO is not an easy material. It is a semiconductor oxide, the properties of which are greatly influenced by external conditions like synthesis methods (Huang et al, 2001; Wu et al, 2002; Elias et al, 2008; Yoshida et al, 2009), temperature (Huang et al, 2007; Guo et al, 2005). Testing atmosphere air, vacuum(Cantu et al, 2006 , 2007 ; Ahn et al, 2007), or illumination (Kenanakis et al, 2008; Feng et al, 2004; Norman et al, 1978), for example ,minimal changes in the shape of the ZnO (nanoparticules, nanorods, nanotips, etc), can produce different properties which in turn , affects the interface with any organic semiconductor or dye molecule.

Moreover, the modification of properties likes hydrophilicity/ hydrophobicity, or the amount of chemisorbed species on the ZnO surface, have already been reported to be affected by UV irradiation. In DSC, a major drawback is associated with the interaction between dye molecules and ZnO itself. Dye loading on ZnO must be carefully controlled in order to obtain the optimal power conversion efficiency for every system.(Chou et al, 2007; Fujishima et al, 1976; Kakiuchi et al, 2006). An excess in loading time results in the formation of aggregates made by the dissociation of the ZnO and the formation of [Zn^{+2} –dye] complexes (Keis et al, 2002; 2000, Horiuchi et al, 2003).

In order to resolve these problems, research is currently focused on the study of new metal-free photosensitizers and the introduction of new anchoring groups (Guillén et al, 2008; Otsuka et al, 2008; Otsuka et al, 2008). Nevertheless, very recent reports indicate that the application of organic dyes could also be affected by factors like high concentration of Li^+ ions in the electrolyte or the photoinduced dye desorption (Quintana et al, 2009). As early as 178, V. J. Norman demonstrated that the absorption of organic dyes, like uranine and rhodamine B, on ZnO can be enhanced under light irradiation. A three- and two –fold increase on the amount of uranine and rhodamine B adsorbed on ZnO, respectively, was obseved after UV- light exposure (Norman et al, 1978). The latter presents important implications in ZnO-besed devices, like solar cells or diodes, since nanostructures layers of ZnO are increasingly being used on these devices, and some research groups have reported on the benefical effect of exposing ZnO-based devices to UV irradiation (Krebs et al, 2008; Verbakel et al, 2007,) .

2.2 TiO_2 presentation

Titanium dioxide is a fascinating material, with a very broad range of different possible properties, which leads to its use in application as different as toothpaste additive. TiO_2 thin films are synthesized for a broad range of different applications, which are summarized below (Estelle, 2002).

2.2.1 Optical coatings

Due to its high index of refraction, TiO_2 has been used for optical applications for more than 50 years (Hass et al, 1952). In particular, it is used as the high index of refraction material in multi-layer interference filtres, as anti reflection coating and as optical wave guides (Pierson, 1999). For many of these application, the mechanical and resistive of the layers are important in addition to the optical properties (Ottermann et al, 1997).

2.2.2 Microelectronics

In electric devices, the scaling down tendency leads to a decrease of the thickness of the gate oxide, which means that for fo the actually used SiO_2 layer, this thickness tends to atomic dimensions. Therefore, other materials are looked at with a higher dielectric constant such that a similar effective capacitance could be obtained with a thicker layer. TiO_2 is one of the promising materials (with Ta_2O_5 and the ternary titanate materials) for this application, due to its high dielectric constant (Pierson, 1999; Boyd et al, 2001).

2.2.3 Gas sensors

Titania fils are known to have sensing properties based on surface interactions of reducing or oxidizing species, which affect the conductivity of the film. Nano-crystalline material was in particular proven to exhibit a very high sensitivity.
Therefore, nano-grain TiO_2 under UV-irradiation is presently widely used as a photo catalyst different applications (water de-pollution (Rabani et al, 1998; Ding et al, 2000; Du et al, 2001), air de-odourization, NO_x decomposition (Negishi et al, 2001), anti-bacteria treatment).

2.2.4 Solar cells

TiO_2 layers are used as photo-anodes in Grätzel's type solar cells,or in a solid state device (Bach et al, 1998). Additionaly, TiO_2 films used as passivation layers on silicon solar cells (Cardarelli, 2000).

2.2.5 Bio-compatible protective layers

Due to their relatively high corrosion resistance and good bio-compatibility, titanium and its alloys are commonly used for biomedical and dental implants. These beneficial properties are believed to be due to the formation of a native protective passive oxide layer. However, there is evidence that this natural layer does not prevent release from titanium in vivo, and therefore, studies have been devoted to deposition of denser, thicker and less oxygen deficient layers to improve the bio-compatibility (Pan et al, 1997). Additionally, TiO_2 was claimed to present good blood compatibility.

2.2.6 Protective and anti-corrosion coatings

Due to its hardness, TiO_2 is used as a protective layer on gold and precious metals (Battiston et al, 1999).

2.2.7 Membrans

TiO_2 coatings are used as membrane materials, with different porosities for different applications.

- Mesoporous membranes are used for ultra filtration or as supports for other Membranes.
- Micro-porous layers are prepared for nano filtration of liquids (Puhlfurss et al, 2000; Benfer et al, 2001).
- Ulra-microporous or dense layers are realized for gaz permselective membranes (Ha et al, 1996). Additionally, the photo catalytic properties of TiO_2 can be used in photo catalytic membrane reactors (Molinari et al, 2001).

2.2.8 As a component of ternary materials

Additionally,titanium dioxide is an important base for all the titanates materials. For instance, (Ba,Sr) TiO_2 which may become important for new geberation dynamic random access memories (Estelle, 2002).

TiO_2 is almost the only material suitable for industrial use at present and also probably in the future. This is because TiO_2 has the most efficient photo activity, the highest stability and the lowest cost (Kokoro et al, 2008). There are two types of photochemical reaction proceeding on a TiO_2 surface when irradiated with ultraviolet light. One includes the photo-induced redex reactions of adsorbed substances, and the other is the photo-induced hydrophilic conversion of TiO_2 itself. The former type has been known since the early part of the 20th centry, but the latter was found only at the end of the century. The combination of these two functions has opened up various novel applications of TiO_2, particularly in the field of building materials (Kokoro et al, 2008).

3. Experimental section

In the present section, we present an experimental comparaison between two dey-Sensitized solar cells based on ZnO nanotube and TiO_2 nanostructures.

First, an aligned ZnO nanotube arrays were fabricated by electrochemical deposition of ZnO anorods followed by chemical etching of the center part of the nanorods. The morphology of the nanotubes can be readily controlled by electrodeposition parameters. By employing the 5.1 μm length nanotubes as photoanodes for DSSC, an overall lightto- electricity conversion efficiency of 1.18% was achieved.

The current–voltage characteristic curves of DSSC fabricated using ZnO nanotubes with different lengths under simulated AM 1.5 light are shown in figure 2(A). The shortcircuit photocurrent densities (I_{sc}) obtained with nanotubes of 0.7, 1.5, 2.9 and 5.1 μm lengths were 0.68, 1.51, 2.50 and 3.24 mA cm−2, respectively. The highest photovoltaic performance of 1.18% (open-circuit voltage Voc = 0.68 V and fill factor FF = 0.58) was achieved for the sample of 5.1 μm length. This efficiency is attractive, taking into account that the film thickness is only 5.1 μm and no scattering layer is added. The Voc of the DSSC decreases upon increasing the length of the ZnO nanotubes, which is possibly related to the increase in the dark current which scales with the surface area of the ZnO film, in agreement with the previous reports on TiO2 nanotube-based DSSC.

The photon-current conversion efficiencies of DSSC using 0.7, 1.5, 2.9 and 5.1 μm length ZnO nanotubes were 0.32%, 0.62%, 0.83% and 1.18%, which were much higher than those of ZnO nanorod DSSCs (i.e. 0.11%, 0.20%, 0.39% and 0.59%). The photocurrent action spectra (figure 2(B)) display the wavelength distribution of the incident monochromatic photon-to-current conversion efficiency (IPCE). Themaximum of IPCE in the visible region is located at 520nm. This is approximately consistent with the expected maximum based on the

accompanying absorption spectrum for the N719 dye (with local maxima at 390 and 535 nm), both corresponding to a metal-to-ligand charge transfer transition.

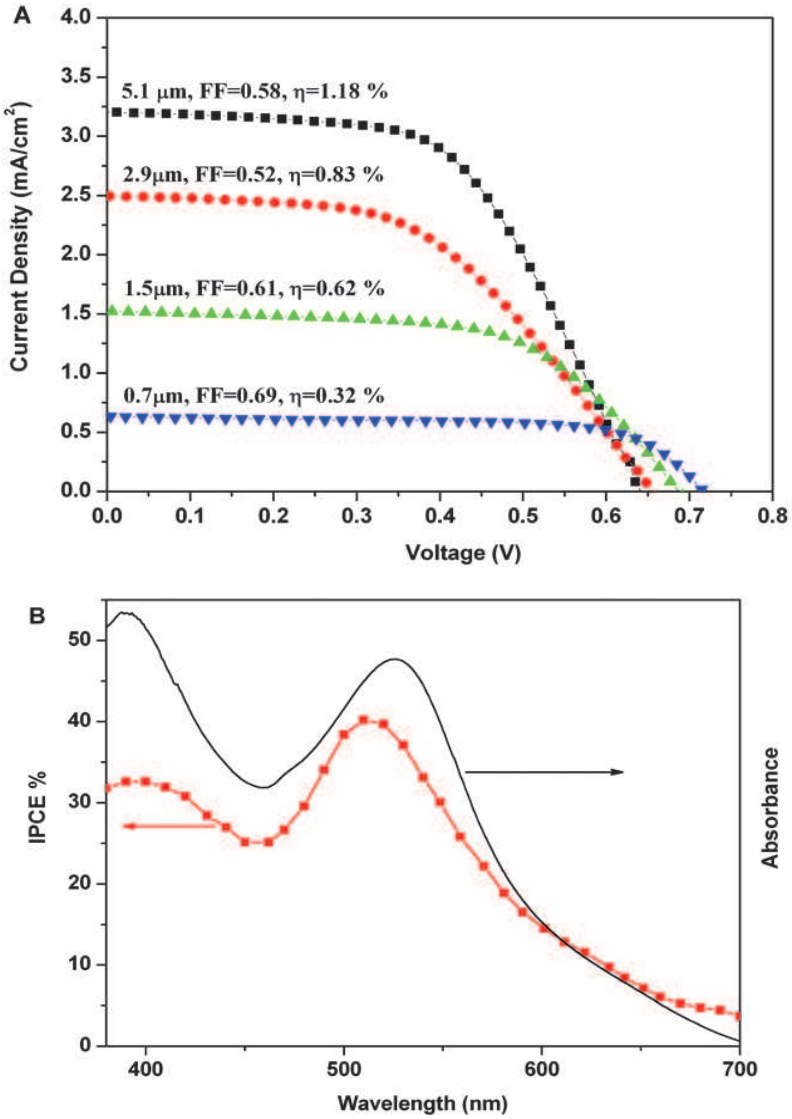

Fig. 2. Performance of the DSSC fabricated using ZnO nanotube array film under full-sun illumination: (A) current–voltage characteristic curves of DSSC with various lengths of ZnO nanotubes with Zn(OAc)2 treatment; (B) incident photon-to-current conversion efficiency (IPCE) of a ZnO nanotube-based device (square) and the absorption spectrum of the N719 dye in solution (solid line).

Second, The DSSCs based on TiO2 nanostructures grown in NaOH solution with different concentrations (0.5, 1, 3, and 10 M) are labeled as 0.5M-DSSC, 1M-DSSC, 3M-DSSC, and 10M-DSSC, respectively. To fabricate DSSCs, the substrates (FTO coated glasses) were first prepared by depositing a thin layer of nanocrystalline TiO2 paste onto FTOs using a screenprinting method. The as-prepared TiO2 membranes were then detached from the Ti plates and adhered onto the substrates as working electrodes. Besides, the DSSC comprised of commercial Degussa P25 TiO2 nanoparticles (labeled as P25-DSSC) was formed using doctor-blading method as a comparison. All of the TiO2 samples were dried under ambient conditions and annealed at 500 °C for 30 min. After cooling, they were chemically treated in a 0.2 M TiCl4 solution at 60 °C for 1 h and then annealed at 450 °C for 30 min to improve the photocurrent and photovoltaic performances. When the temperature decreased to 80 °C, the obtained samples were soaked in 0.3 mM dye solution (solvent mixture of acetonitrile and tert-butyl alcohol in volume ratio of 1:1) and kept for 24 h at room temperature. Here the cis-bis(isothiocyanato) bis (2,20-bipyridyl-4,40-dicarboxylato) ruthenium(II) bis- (tetrabutyl ammonium) (N719) was used as the sensitizer. These dye-coated electrodes were assembled into solar cells with Ptsputtered FTO counter electrodes and the electrolyte containing 0.5 M LiI, 0.05 M I2, and 0.5 M tert-butylpyridine in acetonitrile. photoinduced photocurrent density-voltage (I-V) curves of the constructed solar cells were measured on an electrochemical workstation (model CHI 660C, CH) under an AM 1.5 illumination (100 mW/cm2,model YSS-80A, Yamashita). Electrochemical impedance spectroscopic (EIS) curves of the DSSCs were also observed. The frequency range was from 0.1Hz to 100 kHz. The applied bias voltage was set to the open-circuit voltage (V_{OC}) of the DSSC, which had been determined earlier. The incident photo to current conversion efficiency (IPCE) was detected by the spectral response measuring equipment (CEP-1500, Bunkoh-Keiki. Japan). Figure 3 shows the current density voltage curves of the open cells based on different TiO2 photoelectrodes. The resultant photovoltaic parameters are summarized in Table 2.

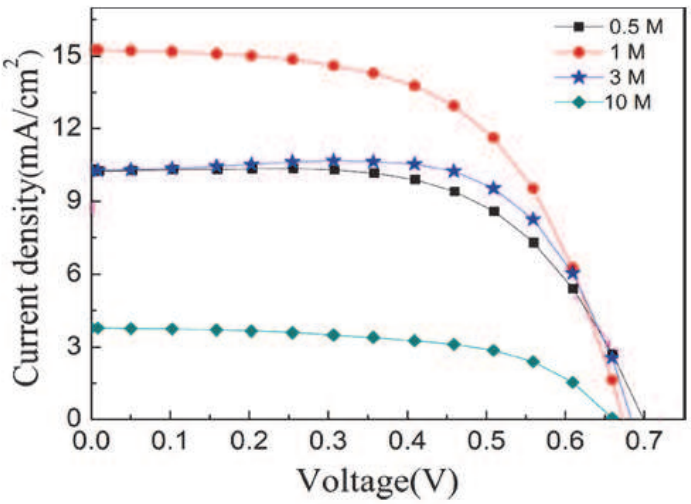

Fig. 3. I-V characteristics of dye-sensitized solar cells assembled with TiO2 films prepared with different concentrations of aqueous NaOH.

The resultant photovoltaic parameters are summarized in Table 1 for ZnO DSSC and in Table 2 for TiO2 DSSC.

Thickness(μm)	V_{oc} (V)	I_{sc} (mA cm^{-2})	FF (%)	η(%)
5.1	0.68	3.24	0.58	1.18
2.9	0.65	2.50	0.52	0.83
1.5	0.70	1.51	0.61	0.62
0.7	0.72	0.68	0.69	0.32

Table 1. Performance Characteristics of DSSCs Based onVarious ZnO nanotube.

DSSCs	V_{oc} (V)	I_{sc} (mA cm^{-2})	FF (%)	η(%)	Thickness(μm)
0.5M-DSSC	0.70	10.26	61.21	4.40	11.68
1M-DSSC	0.67	15.25	58.33	6.00	15.11
3M-DSSC	0.69	10.2	68.87	4.84	24.10
10M-DSSC	0.66	3.71	58.68	1.44	a

Table 2. Performance Characteristics of DSSCs Based on Various TiO2 Nanostructures.

From table 1 and 2, we observe the difference between the photovoltaic performance for these two type DSSC (TiO_2 Nanostructures and ZnO nanotobe), where a high photovoltaic performance is given by TiO_2 Nanostructured with different thickness and over the range of NaOH concentrations, conversion efficient increased from 4.40% at 0.5M to a maximum value of 6.00% at 1 M, which correspond to a high short-circuit photocurrent densities 15.25 mA cm^{-2}. Compared with ZnO nanotube DSSC, where the higher conversion efficient is 1.18% correspond to high short-circuit photocurrent densities 3.24 mA cm^{-2}. The cause of this difference is the based materials properties (ZnO and TiO_2), the method of fabrication and the different condition of measured I-V characteristics of temperature and illumination.

4. Simulation section

Now, to justify the experiment section, we use the computer simulation, which is an important tool for investigating the behaviour of semiconductor devices and for optimising their performance. Extraction and optimisation of semiconductor device parameters is an important area in device modelling and simulation (Chergaar. M et al, 2008; Bashahu M et al, 2007; Priyanka et al, 2007). The current–voltage characteristics of photocells, determined under illumination as well as in the dark, represent a very valuable tool for characterizing the electronic properties of solar cells. The evaluation of the physical parameters of solar cell: series resistance (R_s), ideality factor (n), saturation current (I_s), shunt resistance (R_{sh}) and photocurrent (I_{ph}) is of a vital importance for quality control and evaluation of the performance of solar cells when elaborated and during their normal use on site under different conditions. I-V characteristics of the solar cell can be presented by either a two diode or by a single diode model. Under illumination and normal operating conditions, the single diode model is however the most popular model for solar cells. In this case, the current voltage (I-V) relation of an illuminated solar cell is given by:

$$I = I_{ph} - I_d - I_p = I_{ph} - I_s\left[\exp\left(\frac{\beta}{n}\left(V + IR_s\right)\right) - 1\right] - G_{sh}\left(V + IR_s\right) \quad (1)$$

I_{ph}, I_s, n, R_s and G_{sh} (=1/R_{sh}) being the photocurrent, the diode saturation current, the diode quality factor, the series resistance and the shunt conductance, respectively. I_p is the shunt current and β=q/kT is the usual inverse thermal voltage. The circuit model of solar cell corresponding to equation (1) is presented in figure (4).

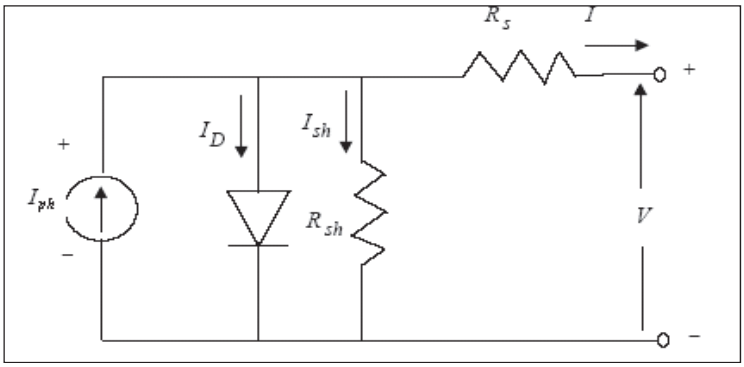

Fig. 4. Equivalent circuit model of the illuminated solar cell.

Determination of R_{sh}

The shunt resistance is considered Rsh = (1 / G_{sh}) >> R_s. the shunt conductance Gsh is evaluated from the reverse or direct bias characteristics by a simple linear fit (Nehaoua. N et al, 2010). The calculated value of G_{sh} gives the shunt current Ip = G_{sh}V.

Determination of n and R_s

Before extracting the ideality factor and the series resistance, our measured I-V characteristics are corrected considering the value of the shunt conductance as obtained from the linear fit and for V+R_sI>>kT, the current voltage relation becomes:

$$I = I_{ph} - I_s\left[\exp\left(\frac{\beta}{n}(V + IR_s)\right)\right] \tag{2}$$

The method concerns directly the usual measured I-V data by writing Eq. (2) in its logarithmic form:

$$\ln\left(I_{ph} - I\right) = \ln I_s + \frac{\beta}{n}(V + IR_s) \tag{3}$$

For a point defined by (V_0, I_0) we have:

$$\ln\left(I_{ph} - I_0\right) = \ln I_s + \frac{\beta}{n}(V_0 + I_0R_s) \tag{4}$$

By subtracting Eq. (3) and Eq. (4) and after a simplification we get a linear equation given by:

$$Y = \frac{\beta}{n}(R_s + X) \qquad \text{For} \quad I >> I_s \tag{5}$$

where:

$$Y = \frac{1}{I - I_0} \ln \frac{(I_{ph} - I)}{(I_{ph} - I_0)} \tag{6}$$

and

$$X = \frac{(V - V_0)}{(I - I_0)} \tag{7}$$

(V_0, I_0) is a point of the I-V curve.
We consider a set of I_i-V_i data giving rise to a set of X-Y values, with i varying from 1 to N. Then, we calculate X and Y values for $I_0 = I_{i0}$ and $I=I_{i0+1}$ up to $I=I_N$. This gives (N-1) pairs of X-Y data. We start again with $I_0 = I_{i0+1}$ and $I = I_{i0+2}$ up to I_N and get (N-2) additional X-Y data, and so on, up to $I_0 = I_{N-1}$. Finally, we obtain N(N-1)/2 pairs of X-Y data that means more values for the linear regression. The linear regression of equation (5) gives n and R_s.

Determination of I_{ph}

For most practical illuminated solar cells we usually consider that $I_s << I_{ph}$, the photocurrent can be given by the approximation $I_{sc} \approx I_{ph}$, where I_{sc} is the short-circuit current. This approximation is highly acceptable and it introduces no significant errors in subsequent calculations (Nehaoua. N et al, 2010).

Determination of I_s

The saturation current I_s was evaluated using a standard method based on the I-V data by plotting $\ln(I_{ph}-I_{cr})$ versus V_{cr} equation (8). Note that I-V data were corrected taking into account the effect of the series resistance.

$$\ln\left(I_{ph} - I_{cr}\right) = \ln\left(I_s\right) + \frac{\beta}{n} V_{cr} \tag{8}$$

When we plot ln (I_c) where ($I_c=I_{ph}-I_{cr}$) versus V_{cr}, it gives a straight line that yields I_s from the intercept with the y-axis.

4.1 Application

The method is applied on the too type of Dey-sensitized solar cell, the first one is based on TiO_2 nanostructures and ZnO nanotube under different condition of fabrication, illumination and temperature. The current-voltage (I-V) characteristics of TiO_2 nanostructures DSSC is taken from the work of (Fang Sho et al, 2010) and The current-voltage (I-V) characteristics of ZnO nanotube is taken from the work of (Jingbin Han et al, 2010). The two characteristics correspond to the higher photovoltaice performance, where η=6.00%, FF=58.33%, I_{sc}=15.25mAcm^{-2} and V_{oc}=0.67V for TiO_2 nanostructures, and for ZnO nanotube η=1.18%, FF=0.58%, I_{sc}=3.24mAcm^{-2} and V_{oc}=0.68V.

4.2 Results and discussion

The shunt conductance $G_{sh} = 1 / R_{sh}$ was calculated using a simple linear fit of the reverse or direct bias characteristics. The series resistance and the ideality factor were obtained from the linear regression (5) using a least square method.

In order to test the quality of the fit to the experimental data, the percentage error is calculated as follows:

$$e_i = \left(I_i - I_{i,cal}\right)\left(100 / I_i\right) \tag{9}$$

Where $I_{i,cal}$ is the current calculated for each V_i, by solving the implicit Eq.(1) with the determined set of parameters (I_{ph}, n, R_s, G_{sh}, I_s). (I_i, V_i) are respectively the measured current and voltage at the ith point among N considered measured data points avoiding the measurements close to the open-circuit condition where the current is not well-defined (Chegaar M et al, 2006).

Statistical analysis of the results has also been performed. The root mean square error (RMSE), the mean bias error (MBE) and the mean absolute error (MAE) are the fundamental measures of accuracy. Thus, RMSE, MBE and MAE are given by:

$$\begin{aligned} RMSE &= \left(\sum |e|_i^2 / N\right)^{1/2} \\ MBE &= \sum e_i / N \\ MAE &= \sum |e|_i / N \end{aligned} \tag{10}$$

N is the number of measurements data taken into account.

The extracted parameters obtained using the method proposed here for the Dey-Sensitized solar cell based on TiO2 nanostructures and ZnO nanotube are given in Table 3. Satisfactory agreement is obtained for most of the extracted parameters. good agreement is reported. Statistical indicators of accuracy for the method of this work are shown in Table 3.

	DSSC-TiO_2 nanostructures	DSSC-ZnO nanotube
G_{sh} (Ω^{-1})	0.001269	0.000588
R_s (Ω)	0.025923	0.383441
n	1.629251	3.560949
I_s(μA)	0.33556	0.16553
I_{ph}(mA/cm^2)	15.99	3.25
RMSE	0.850353	1.875871
MBE	0.232276	0.727544
MAE	0.757886	1.053901

Table 3. Extracted parameters for Dey-Sensitized solar cell based on TiO_2 nanostructures and ZnO nanotube.

Figures 5 and 6 show the plot of I-V experimental characteristics and the fitted curves derived from equation (1) with the parameters shown in Table 3 for Dey-Sensitized solar cell based on TiO_2 nanostructures and ZnO nanotube. The interesting point with the procedure described herein is the fact that we do not have any limitation condition on the voltage and it is reliable, straightforward, easy to use and successful for different types of solar cells.

Extracting solar cells parameters is a vital importance for the quality control and evaluation of the performance of the solar cells, this parameters are: series resistance, shunt conductance, saturation current, the diode quality factor and the photocurrent. In this work, a simple method for extracting the solar cell parameters, based on the measured current-voltage data. The method has been successfully applied to dey-Sensitized solar cell based on TiO_2 nanostructures and ZnO nanotube under different temperatures.

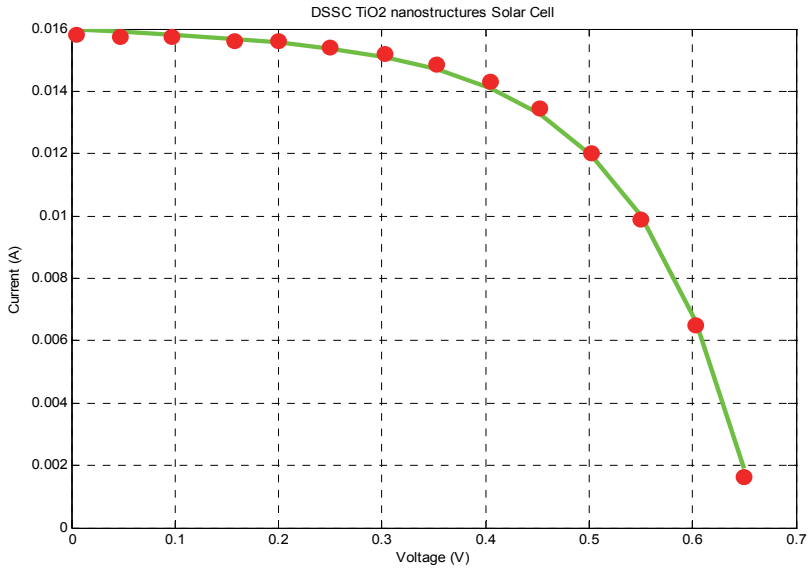

Fig. 5. Experimental (●) data and fitted curve of TiO_2 nanostructures DSSC.

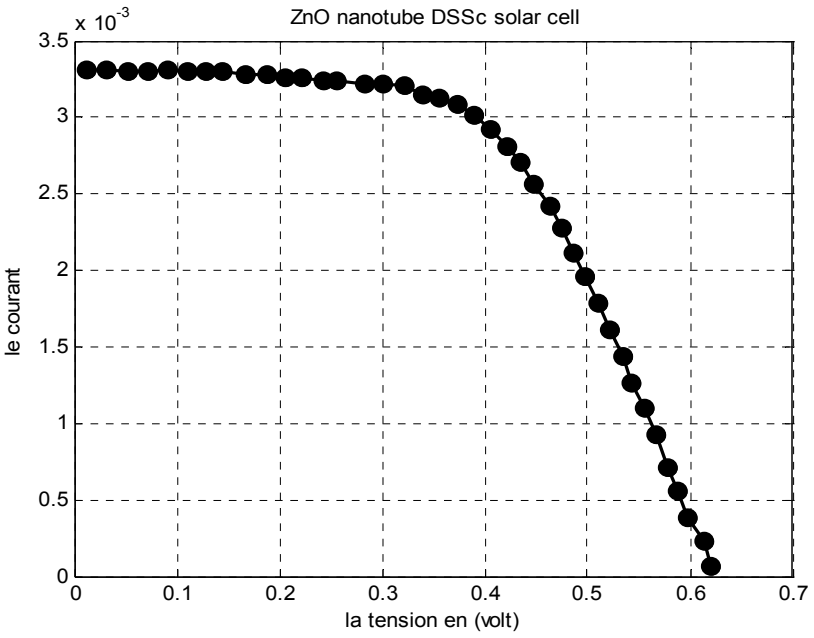

Fig. 6. Experimental (●) data and fitted curve of ZnO nanotube DSSC.

Figures 5 and 6 shows the plot of I–V experimental characteristics and the fitted curves derived from equation (1) with the parameters shown in Table 3 for the dey-Sensitized solar cell based on TiO_2 nanostructures and ZnO nanotube solar cell. Good agreement is observed for the different structure, especially for the TiO_2 nanostructures solar cells with statistical error less than 1%, and 2% for ZnO nanotube DSSC solar cells respectively, which attribute mainly to lower parasitic losses, where we can observe a low series resistance 0.025923Ω compared to 0.383441 Ω for TiO_2 nanostructures and ZnO nanotube solar cell respectively.
The interesting point with the procedure described herein is the fact that we do not have any limitation condition on the voltage and it is reliable, straightforward, easy to use and successful for different types of solar cells.

5. Conclusion

In this contribution, a simple comparative study between experimental and simulation works to improve the dey-sensitized solar cell performance of two DSSCs based on TiO_2 nanostrucures and ZnO nanotube, under differents condition of temperature. We compare the different parameters which are: the conversion efficient, the fill factor, the short-circuit photocurrent and the open-circuit voltage, where we observe a high photovoltaic performance for TiO_2 nanostrucures with maximun conversion efficient 6% compared to 1.18% for ZnO nanotube. In second time, an evaluation of the physical parameters of solar cell: series resistance (R_s), ideality factor (n), saturation current (I_s), shunt resistance (R_{sh}) and photocurrent (I_{ph}) from measured current-voltage characteristics by using a numerical method proposed by th authors. Extracting solar cells parameters is a vital importance for the quality control and evaluation of the performance of solar cells when elaborated and during their normal use on site under different conditions. Good resuts are given by the differents DSSCs, and specialy for on dey-sensitized TiO_2 nanostrucures, which justify the experimental work.

6. References

Boyd, I. W. & Zhang, J. Y. (2001), *Solid-State Electronics*, 45, 1413
Benfer, S.; Popp, U.; Richter, H. et al.(2001) *Separation and Purification Technology*, 22-23. 231.
Bashahu M, Nkundabakura P. Solar energy 2007; 81:856-863.
Bach,U. ; Lupo, D. ;Comte, P. et al.(1998), *Nature*,395 ,583.
Battiston, G., A. ; Gerbasi, R. ; Porchia, M. et al. (1999), *Chemical Vapor Deposition*,5 ,73
Chang Y.; Teo, J. J. ; Zeng, H. C. (2005), *Langmuir*. 21(3), 1074-1079, 21(3), 1074-1079
Cao, Q. H. ; Gao, Y. Q. ; Chen, X. Y. ; Mu, L. ; Yu, W. C. & Qian, Y. T.(2006). *Chem. Lett.* 35(2), 178-179.
Cao, X. B. ; Gu, L. ; Zhuge, L. ; Gao, W. J.; Wang, W. C. & Wu, S. F.(2006) *Adv. Funct. Mater.* 16(7), 896-902.
Chegaar M, Nehaoua. N, Bouhemadou. A. Energy conversion and management 2008, 49:1376-1379.
Chegaar M, Azzouzi G, Mialhe P. Solid State Electronics 2006; 50:1234-1237.
Chen, W.; Lu, Y. H. ; Wang, M. ; Kroner, L. ; Paul, H. ; Fecht, H.J.; Bednarcik, J.; Stahl, K.; Zhang, Z. L.; Wiedwald, U.; Kaiser, U.; Ziemann.,P.; Kikegawa, T.; Wu, C. D. & Jiang, J. Z. J.(2009) *Phys. Chem. C* , 113(4),1320-1324.
Cardarelli, F.(2000), *in Materials Handbook A Concise Desktop Reference*(Springler-Verlag).

Dinsmore, A. D.; Hsu, M. F.; Nikolaides, M. G.; Marquez, M.;Bausch, A. R. & Weitz, D. A.(2002) *Science*, 298(5595),1006-1009.

Ding, Z. ; Hu, X. ; Lu, G. Q. ; et al.(2000), *Langmuir*, 16 ,6216.,

Du, G., H. ; Chen, Q. ; Che, R. C. et al. (2001), *Appl. Phys. Lett*., 79 ,3702

Estelle Wagner (2002), thesis(selective light induced chemical vapour deposition of titanium dioxide thin films), EPFL, 2650.

Engeneering Chemical Research, (199), 3381

Elias, J.; Tena-Zaera, R. & Lévy-Clément, C.(2008*), J. Phys. Chem. C*, 112, 5736.

Fujishima,A.; Iwase, T. & Honda,K. J. Am, J.(1976). *Chem. Soc*., 98(6), 1625.

Fan, H. j.; Werner, P. & Zacharias, M.(2006) Small. 2(6),700.

Fang shao, Jing sun, lian gao, Songwang, Jianqiang luo. Physical chemestry C. Dx.doiorg/10.1021/jp110743m.

E. Guillén et al. J. Phtochem. Photobiol., A., 2008,200,364.,

I. Gonzalez-Valls and M. Lira-Cantu.(2009), *Energy Environ*. Sci. 2,1

L. E. Greene,M. Law, J. Goldberger, F. Kim, J. C. Johnson,Y. Zhang, R. J. Saykally and P. D. Yang, Angew.(2003). Chem., Int. Ed., 42(26), 3031.

Guo, M.; Diao, P. and Cai, S. M. (2005), *J. Solid State Chem*. 178, 1864

Huang, M. H.; Mao,S. ;Feick, H.;Yan, H. Q.; Wu, Y. Y.; Kind, H.; Weber, E. Russo, & Yang, P. D.(2001), *Science*, 292, 1897.,

Hass, G. Vacuum, 11,(1952),331

Huang, J. H.; Gao, L.(2006), *J. Am. Ceram. Soc*. 89(12), 3877-3880.

Hsu, C. C.; Wu, N. L. (2005), *Photochem. Phtobiol. A* 172(3), 269-274.),

Horiuchi,H.; Katoh,R.; Hara, K. Yanagida, M.; Murata, S. Arakawa, H. & Tachiya, M.(2003), *J. Phys. Chem*. B, 107, 2570.

Ha, Y. H., Nam, S. W. ; S. W., ; Lim, T. H. L. et al.(1996), *Journal of Membrane Science*, 111, 81.

Ishizumi, A. & Kanemitsu, Y. (2005): *Appl. Phys. Lett*. 86(253106).

Ishizumi, A.; Y. Taguchi, Yamamoto, A. & Kanemitsu, Y.(2005): *Thin Solid Films* 486(50).

Ibarra. L. & Alzorriz, M. J.(2002), *Appl. Polym. Sci*. 84(3), 605-615.

Ibarra, L. ; Macros-Fernandez, A. & Alzorriz., M.(2002), *Polymer*, 43(5), 1649-1655.

Ibarra, L. & Alzorriz, M. (2002), *J. Appl. Polym. Sci*., 86(2), 335-340.

Ito, S., Zakeeruddin, S. M., Humphry-Baker, R., Liska, P., Charvet, R., Comte,P., Nazeeruddin, M., Péchy, P., Takata, M., Miura, H., Uchida, S. &Grätzel 2006, 'High-efficiency organicdye sensitized solar cells controlled by nanocrystalline-TiO2 electrodethickness,' *Adv. Mater*. 18, p. 1202.

Jain A, Kapoor A. Solar energy mater solar cells 2005; 86:197-205

Jingbin Han, Fengru Fan, chen xu, Shisheng Lin, Min wei, Xue duan, Zhong lin wang. Nanotechnology 2010, 21:405203(7p).

Janne Halme, thesis (2002), *Dye-sensitized nanostructured and organic photovoltaic cells: technical review and preliminary test*s, HELSINKI UNIVERSITY OF TECHNOLOGY.

Krebs, F. C. (2008*), Sol. Energy Mater. Sol. Cells*, 92,715.

Keis, K.; Bauer, C.; Boschloo, G.; Hagfeldt, A.; Westermark, K.; Rensmo, H. & Siegbahn, H.(2002), *J. Photochem. Photobiol., A*, 148.57 .

Keis, K.; Magnusson, E.; Lindström, H.; Lindquist, S. E. & Hagfeldt, A.(2002), *Sol. Energy Mater. Sol. Cells,* 73, 51.

Kakiuchi, K.; Hosono, E. & Fujihara, S.(2006). *J. Photochem. Photobiol. A* 179, 81.

Keis, K.; Lindgren, J.; S. E. Lindquist, S. E. & Hagfeldt, A.(2000), *Langmuir*, 16, 4688.
Kokoro et al. Appl. Phys. Express 1 (2008) 081202
Li, Z. Y.; Kobayashi, N.; Nishimura, A. & Hasatani.(2005), *M. Chem. Eng.Commun*. 12(7) ,18-932.
Liang, H. P.; Zhang, H. M.; Hu, J. S.; Guo, Y. G.; Wan, L. J.& Bai,C. L. Angew.(2004) *Chem., Int. Ed*. 43(12), 1540-1543.
Lee, K. T.; Jung, Y. S.; Oh, S. M.(2003), J. Am. Chem. Soc. 125(19), 5652-5653
Liu,X. M. ; Yin, W. D. ; Miao, S. B. & Ji, B. M.(2009). Mater. Chem. Phys. 113(2-3), 518-522
Li,B. X. ; Rong, G. X. ; Xie, Y. ; Huang, L. F. & Feng, C. Q.(2006), Inorg. Chem., 45(16), 6404-6410.
Liu, X. Y. ; Xi, G. C. ; Liu, Y. K. ; Xiong, S. L. ; Chai, L. L. & Qian, Y. T.(2007) *J. Nanosci. Nanotechnology*. 7(12), 4501-4507
Lou, X. W.; Archer, L. A. & Yang, Z. C.(2008), *Adv. Matter*. 20(21), 3987-4019.
Li, Z. Y.; Kobayashi, N.; Nishimura, A. & Hasatani, M.(2005), *Chem. Eng.Commun*. 12(7) ,18-932.
Lin, X. X. ; Zhu, Y. F. & Shen, W. Z.(2009), *J. Phys. Chem. C*, 113(5), 1812-1817 ,113(5), 1812-1817
Lira-Cantu, M. & Krebs, F. C.(2006), *Sol. Energy Mater. Sol. Cells*, 90,2076.
Lira-Cantu, M.; Norman, K.; Andreasen, J. W.; Casan-Pastor, N. & Krebs, F. C.(2007), *J. Electrichem. Soc*. 154(6), B508
Lira-Cantu, M.; Norrman, K.; Andreasen, J. W.& Krebs, F. C. (2006), Chem. Mater., 18, 5684.,
Molinari, R. ; Grande, C. ; Drioli, E. et al. (2001), *Catalysis Today*, 67,1.
Myo Than HTAY,; Minori ITOH,; Yoshio HASHIMOTO,& Kentaro ITO(2008),J. *Appl. Phys*. (47)541
Negishi, N. & Takeuchi, K.(2001), *Thin Sold Films*, 392, 249.
Norman, V. j.(1978), *Australian J. Chem*., 25(6),1189.
Nehaoua N, Chergui Y , Mekki D E. Vacuum 2010 , 84 : 326–329.
Otsuka, A.; K. Funabiki, Sugiyama,N.; Mase, H.; T. Yoshida,T.; Minoura, H. & Matsui, M.(2008), *Chem. Lett*. 37(2), 176.
Ottermann, C. R. ; Ottermann, R. ;Kischnereit,R. ; Anderson, O. et al.(1997), *Mat. Res. Soc. Symp. Proc*., 436 ,251
Otsuka et al. Dalton Trans., 2008,5439
Pan, J.; Leygraf, C.; Thierry, D. et al.(1997), *Journal of Biomedical Materials Research*, 35, ,309.
Pierson, H. O.(1999), *Handbook of chemical vapour deposition(CVD)*: *principles, technology and applications*, 2nd ed.(Park Ride, 1999).
Puhlfurss, P. ; Voigt, A. ; Weber, R. et al. (2000), *Journal of Membrane Science*, 174, 123.
Priyanka, Lal M , Singh S N. Solar energy material and solar cells 2007; 91:137-142.
Quintana,M.; Edvinsson,T.; Hagfeldt, A. & Boschloo, G.(2007), *J. Phys.Chem. C*. 111, 1035
Quintana, M.; Marinado, T.; Nonomura,K.; Boschloo, G. & Hagfeldt, A.(2009), J. *Photochem. Photobiol*. *A*, 202,159
Rabani, J.; Yamashita, K. ; Ushida K. et al. (1998). *J. Phys. Chem*., 102, 1689.
K. Sakurai, T. Takagi, T. Kubo, D. Kajita, T. Tanabe, H. et al. J. Cryst. Growth 237-239(2002)514.
F. Verbakel, S. C. J. Meskers and R. A. J. Janssen.(2007), *J. Phys. C*, 111,10150
Verbakel,F.; Meskers, S. C. J. & Janssen, R. A. G..(2007), *J. Appl. Phys*. 102(8), 083701
Yamamoto, A. ; Atsuta S.; & Y. Kanemitsu, Y.(2005) ; *J. Lumin*, 112 (169).
Yamamoto,A., S. Atsuta, & Kanemitsue, Y.(2005): *Physica E* 26(96).
Wu, J. J. & Liu, S. C. (2002), *Adv. Mater*. 14(3), 215.

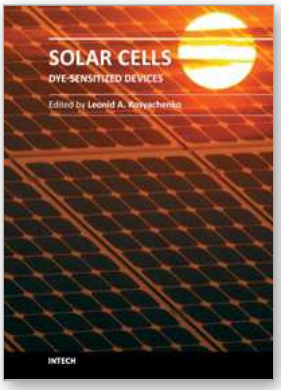

Solar Cells - Dye-Sensitized Devices
Edited by Prof. Leonid A. Kosyachenko

ISBN 978-953-307-735-2
Hard cover, 492 pages
Publisher InTech
Published online 09, November, 2011
Published in print edition November, 2011

The second book of the four-volume edition of "Solar cells" is devoted to dye-sensitized solar cells (DSSCs), which are considered to be extremely promising because they are made of low-cost materials with simple inexpensive manufacturing procedures and can be engineered into flexible sheets. DSSCs are emerged as a truly new class of energy conversion devices, which are representatives of the third generation solar technology. Mechanism of conversion of solar energy into electricity in these devices is quite peculiar. The achieved energy conversion efficiency in DSSCs is low, however, it has improved quickly in the last years. It is believed that DSSCs are still at the start of their development stage and will take a worthy place in the large-scale production for the future.

INTECH
open science | open minds

InTech Europe
University Campus STeP Ri
Slavka Krautzeka 83/A
51000 Rijeka, Croatia
Phone: +385 (51) 770 447
Fax: +385 (51) 686 166
www.intechopen.com

InTech China
Unit 405, Office Block, Hotel Equatorial Shanghai
No.65, Yan An Road (West), Shanghai, 200040, China
中国上海市延安西路65号上海国际贵都大饭店办公楼405单元
Phone: +86-21-62489820
Fax: +86-21-62489821